Cylindrical Couette flows of a rarefied gas with evaporation and condensation: Reversal and bifurcation of flows (Researches on Rotating Fluids)

AUTHOR(S):

Sone, Yoshio; Sugimoto, Hiroshi; Aoki, Kazuo

CITATION:

Sone, Yoshio ...[et al]. Cylindrical Couette flows of a rarefied gas with evaporation and condensation: Reversal and bifurcation of flows (Researches on Rotating Fluids). 数理解析研究所講究録 1999, 1075: 37-52

ISSUE DATE:

1999-01

URL:

http://hdl.handle.net/2433/62626

数理解析研究所講究録
1075巻 1999年 37-52

蒸発・凝縮を伴う希薄気体のCouette流: 流れの逆転と分岐

Cylindrical Couette flows of a rarefied gas with evaporation and condensation: Reversal and bifurcation of flows

京大・工・航空宇宙　　曾根 良夫, 杉元 宏, 青木 一生

Yoshio Sone, Hiroshi Sugimoto, and Kazuo Aoki

Department of Aeronautics and Astronautics, Graduate School of Engineering, Kyoto University, Kyoto 606-8501, Japan

A rarefied gas between two coaxial circular cylinders made of the condensed phase of the gas is considered, where each cylinder is kept at a uniform temperature and is rotating at a constant angular velocity around its axis (cylindrical Couette flows of a rarefied gas with evaporation or condensation on the cylinders). The steady behavior of the gas, with special interest in bifurcation of a flow, is studied on the basis of kinetic theory from the continuum to the Knudsen limit. The solution shows profound variety: reversal of direction of evaporation-condensation with variation of the speed of rotation of the cylinders; contrary to the conventional cylindrical Couette flow without evaporation and condensation, bifurcation of a flow in a simple case where the state of the gas is circumferentially and axially uniform.

1 Introduction

Bifurcation of flows attracts many scientists and engineers, and a lot of works have been done in the framework of classical gas dynamics, especially in relation to turbulence.[1–9] Bénard and Taylor-Couette flows are its most well-known examples. The study of these flows for a rarefied gas is also being done in recent years.[10–14]

In this paper we will present a new example of bifurcation of a simple flow, which is found in a rarefied gas as well as in a gas in the continuum limit. That is, we consider a gas between two coaxial circular cylinders made of the condensed phase of the gas, on the surface of which evaporation or condensation thus may take place. Each cylinder is kept at a uniform temperature and is rotating at a constant angular velocity around its axis. We investigate the behavior of the gas (cylindrical Couette flows of a rarefied gas with evaporation or condensation on the cylinders) under the condition that the state of the gas is axially and circumferentially uniform on the basis of kinetic theory from the continuum to the Knudsen limit. The centrifugal force induced in the gas by rotation of the cylinders affects evaporation and condensation on the cylinders, and this introduces profound variety of the behavior of the gas. In the following analysis, we find reversal of direction of evaporation-condensation with variation of the speed of rotation of the cylinders and bifurcation of a flow in the simple case where the state of the gas is circumferentially and axially uniform, contrary to the conventional cylindrical Couette flow without evaporation and condensation.

2 Problem and basic equation

Consider a rarefied gas between two coaxial circular cylinders made of the condensed phase of the gas, where each cylinder is kept at a uniform temperature and is rotating at a constant angular velocity around its axis. Let the radius, temperature, and circumferential velocity of the surface of the inner cylinder be L_1, T_1, and $V_{\theta 1}$, respectively; let the corresponding quantities of the outer cylinder be L_2, T_2, and $V_{\theta 2}$. The saturation gas pressure at temperature T (or T_1, T_2) is denoted by p_s (or p_{s1}, p_{s2}). The Knudsen number Kn of the system is defined by l_1/L_1, where l_1 is the mean free path of the gas molecules in the equilibrium state at rest with pressure p_{s1} and temperature T_1. We will investigate the steady behavior of the gas under the following assumptions: i) The behavior of the gas is described by the Boltzmann-Krook-Welander equation (BKW or BGK equation).[15–18] Notes on the generalization of the result for the standard Boltzmann equation will be given in several places. ii) The velocity distribution of the gas molecules leaving the inner (or outer) cylinder is the corresponding part of the Maxwellian distribution with pressure p_{s1} (or p_{s2}), circumferential velocity $V_{\theta 1}$ (or $V_{\theta 2}$), and temperature T_1 (or T_2). (This is called the complete condensation condition on the interface of a gas and its condensed phase.[18–20]) iii) The behavior of the gas is axially and circumferentially uniform. Then the axial velocity vanishes.

The Boltzmann-Krook-Welander equation for a steady flow with axial and circumferential uniformity is given in the cylindrical coordinate system (r, θ, z), with the axis of the cylinder as the z axis (Fig. 1), as follows:

$$\xi_r \frac{\partial f}{\partial r} + \frac{\xi_\theta^2}{r}\frac{\partial f}{\partial \xi_r} - \frac{\xi_r \xi_\theta}{r}\frac{\partial f}{\partial \xi_\theta} = A_{col}\rho(f_e - f), \quad (1)$$

$$f_e = \frac{\rho}{(2\pi RT)^{3/2}} \exp\left(-\frac{(\xi_r - u_r)^2 + (\xi_\theta - u_\theta)^2 + \xi_z^2}{2RT}\right), \quad (2)$$

$$\rho = \iiint f d\xi_r d\xi_\theta d\xi_z, \quad (3a)$$

$$\rho u_r = \iiint \xi_r f d\xi_r d\xi_\theta d\xi_z, \quad (3b)$$

$$\rho u_\theta = \iiint \xi_\theta f d\xi_r d\xi_\theta d\xi_z, \quad (3c)$$

$$3R\rho T = \iiint[(\xi_r - u_r)^2 + (\xi_\theta - u_\theta)^2 + \xi_z^2]f \, d\xi_r d\xi_\theta d\xi_z, \quad (3d)$$

$$p = R\rho T, \quad (3e)$$

where ξ_r, ξ_θ, and ξ_z are, respectively, the radial (r), azimuthal (θ), and axial (z) components of the molecular velocity; f is the velocity distribution function of the gas molecules, which is a function of r, ξ_r, ξ_θ, and ξ_z; ρ is the density of the gas; u_r and u_θ are, respectively, the radial and circumferential components of the flow velocity, which are its nonvanishing components; T is the temperature of the gas; p is the pressure of the gas; A_{col} is a constant; R is the specific gas constant (or the Boltzmann constant divided by the mass of a gas molecule). The integrations in Eqs. (3a)–(3d), and in what follows unless otherwise stated, are carried out over the range ($-\infty < \xi_r < \infty$, $-\infty < \xi_\theta < \infty$, $-\infty < \xi_z < \infty$). The $A_{col}\rho$ is the collision frequency of a gas molecule, which is independent of molecular velocity for the BKW equation.

The complete condensation boundary conditions on the cylinders are given as follows: on the inner cylinder ($r = L_1$),

$$f = \frac{\rho_{s1}}{(2\pi RT_1)^{3/2}} \exp\left(-\frac{\xi_r^2 + (\xi_\theta - V_{\theta 1})^2 + \xi_z^2}{2RT_1}\right) \quad (\xi_r > 0), \quad (4)$$

where

$$\rho_{s1} = p_{s1}/RT_1, \quad (5)$$

and on the outer cylinder ($r = L_2$),

$$f = \frac{\rho_{s2}}{(2\pi RT_2)^{3/2}} \exp\left(-\frac{\xi_r^2 + (\xi_\theta - V_{\theta 2})^2 + \xi_z^2}{2RT_2}\right) \quad (\xi_r < 0), \quad (6)$$

where

$$\rho_{s2} = p_{s2}/RT_2. \quad (7)$$

For the convenience of analysis, we introduce the following nondimensional variables (Fig. 1) and marginal velocity distribution functions:

$$r = L_1\hat{r}, \quad (8a)$$

$$\xi_r = (2RT_1)^{1/2}\zeta\cos\theta_\zeta,$$

$$\xi_\theta = (2RT_1)^{1/2}\zeta\sin\theta_\zeta, \quad (8b)$$

$$\xi_z = (2RT_1)^{1/2}\zeta_z,$$

$$\rho = \rho_{s1}\hat{\rho}, \quad u_r = (2RT_1)^{1/2}\hat{u}_r,$$

$$u_\theta = (2RT_1)^{1/2}\hat{u}_\theta, \quad p = p_{s1}\hat{p}, \quad T = T_1\hat{T}, \quad (8c)$$

$$\begin{bmatrix} g \\ h \end{bmatrix} = \frac{2RT_1}{\rho_{s1}} \int_{-\infty}^{\infty} \begin{bmatrix} 1 \\ \xi_z^2/2RT_1 \end{bmatrix} f d\xi_z. \quad (8d)$$

With these new variables, the BKW equation (1) is reduced to

$$D\begin{bmatrix} g \\ h \end{bmatrix} = \frac{2}{\sqrt{\pi}\mathrm{Kn}}\hat{\rho}\left(\begin{bmatrix} g_e \\ h_e \end{bmatrix} - \begin{bmatrix} g \\ h \end{bmatrix}\right), \quad (9)$$

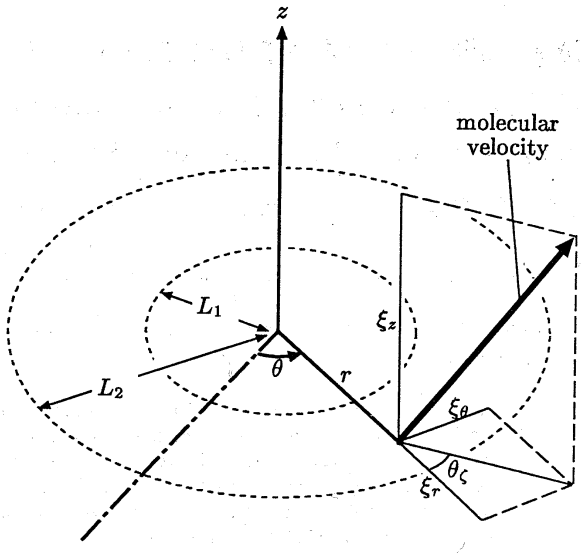

Fig. 1. Coordinate systems.

where

$$D = \zeta\cos\theta_\zeta\frac{\partial}{\partial\hat{r}} - \frac{\zeta\sin\theta_\zeta}{\hat{r}}\frac{\partial}{\partial\theta_\zeta}, \quad (10a)$$

$$\mathrm{Kn} = \frac{l_1}{L_1}, \quad l_1 = \frac{(8RT_1/\pi)^{1/2}}{A_{col}\rho_{s1}}, \quad (10b)$$

$$\begin{bmatrix} g_e \\ h_e \end{bmatrix} = \frac{\hat{\rho}}{\pi}\begin{bmatrix} 1/\hat{T} \\ 1/2 \end{bmatrix} \times\exp\left(-\frac{\zeta^2 + \hat{u}_r^2 + \hat{u}_\theta^2 - 2\hat{u}_r\zeta\cos\theta_\zeta - 2\hat{u}_\theta\zeta\sin\theta_\zeta}{\hat{T}}\right). \quad (10c)$$

The l_1 is the mean free path of the gas molecules in the equilibrium state at rest with pressure p_{s1} and temperature T_1, and Kn is the Knudsen number at the state. By the introduction of the marginal velocity distributions g and h, the variable ζ_z is eliminated, and in the new independent variables ($\hat{r}$, ζ, θ_ζ), the equations for g and h contain only the derivatives with respect to $\hat{r}$ and θ_ζ.

The macroscopic variables $\hat{\rho}$, $\hat{u}_r$, $\hat{u}_\theta$, and $\hat{T}$ are expressed by g and h as

$$\hat{\rho} = \iint \zeta g d\zeta d\theta_\zeta, \quad (11a)$$

$$\hat{u}_r = \frac{1}{\hat{\rho}}\iint \zeta^2\cos\theta_\zeta g d\zeta d\theta_\zeta, \quad (11b)$$

$$\hat{u}_\theta = \frac{1}{\hat{\rho}}\iint \zeta^2\sin\theta_\zeta g d\zeta d\theta_\zeta, \quad (11c)$$

$$\frac{3}{2}\hat{T} = \frac{1}{\hat{\rho}}\iint \zeta(\zeta^2 g + h)d\zeta d\theta_\zeta - \hat{u}_r^2 - \hat{u}_\theta^2. \quad (11d)$$

The two-fold integrations with respect to ζ and θ_ζ in Eqs. (11a)–(11d), and in what follows unless otherwise stated, are carried out over the domain ($0 \le \zeta < \infty$, $-\pi < \theta_\zeta \le \pi$).

The boundary conditions are, at $\hat{r} = 1$,

$$\begin{bmatrix} g \\ h \end{bmatrix} = \frac{1}{\pi}\begin{bmatrix} 1 \\ \frac{1}{2} \end{bmatrix} \exp\left(-\zeta^2 - \frac{V_{\theta 1}^2}{2RT_1} + \frac{2V_{\theta 1}\zeta \sin\theta_\zeta}{(2RT_1)^{1/2}}\right) \quad (|\theta_\zeta| < \pi/2), \tag{12}$$

and at $\hat{r} = L_2/L_1$,

$$\begin{bmatrix} g \\ h \end{bmatrix} = \frac{1}{\pi}\frac{p_{s2}T_1}{p_{s1}T_2}\begin{bmatrix} T_1/T_2 \\ 1/2 \end{bmatrix} \times \exp\left(-\frac{T_1}{T_2}\left(\zeta^2 + \frac{V_{\theta 2}^2}{2RT_1} - \frac{2V_{\theta 2}\zeta \sin\theta_\zeta}{(2RT_1)^{1/2}}\right)\right) \quad (\pi/2 < |\theta_\zeta| \le \pi). \tag{13}$$

The problem is determined by the six parameters Kn, L_2/L_1, $V_{\theta 1}/(2RT_1)^{1/2}$, $V_{\theta 2}/(2RT_1)^{1/2}$, p_{s2}/p_{s1}, and T_2/T_1. We will analyze this boundary-value problem mainly numerically for various sets of values of these parameters. The saturation gas pressure p_s is generally a rapidly increasing function of temperature T. For many gases, $p_{s2}/p_{s1} = 1.2$, for example, corresponds to $1 < T_2/T_1 < 1.02$; thus, it is sufficient to take $T_2/T_1 = 1$ in illustrative examples.

3 Outline of method of numerical solution

The numerical analysis of the boundary-value problem (9), (12), and (13) will be carried out by a finite-difference method. We studied a cylindrical problem in Refs. 21 and 22, where steady evaporation of a rarefied gas from a stationary cylindrical condensed phase into an infinite expanse of the gas with various pressures or into a vacuum was considered. We can make use of the finite-difference method developed in Ref. 21. Thus, we only outline the method here.

(i) We consider the problem in a finite domain ($1 \le \hat{r} \le L_2/L_1$, $0 \le \zeta \le \zeta_D$, $-\pi \le \theta_\zeta \le \pi$) in ($\hat{r}$, ζ, θ_ζ) space, where ζ_D is chosen properly depending on the situations. From our numerical tests, g and h are seen to decay rapidly with ζ, and therefore accurate computation of the problem can be carried out with reasonable size of ζ_D. The discrete solution ($g_\#$, $h_\#$) of (g, h) at the lattice points in ($\hat{r}$, ζ, θ_ζ) space is constructed as the limit of the sequence ($g_\#^{(n)}$, $h_\#^{(n)}$) obtained as follows. The initial solution ($g_\#^{(0)}$, $h_\#^{(0)}$) of the iteration process is chosen properly. Let the solution ($g_\#^{(n)}$, $h_\#^{(n)}$) be known. The solution ($g_\#^{(n+1)}$, $h_\#^{(n+1)}$) in ($-\pi \le \theta_\zeta < -\pi/2$) and ($\pi/2 < \theta_\zeta \le \pi$) is computed successively from $\hat{r} = L_2/L_1$ to $\hat{r} = 1$ (the solution in domains I_1 and I_2 in Fig. 2) and then ($g_\#^{(n+1)}$, $h_\#^{(n+1)}$) in ($-\pi/2 < \theta_\zeta < \pi/2$) from $\hat{r} = 1$ to $\hat{r} = L_2/L_1$ (the solution in domains II_1 and II_2 in Fig. 2) with the aid of a finite-difference equation for Eq. (9). In the computation of ($g_\#^{(n+1)}$, $h_\#^{(n+1)}$) in the domain I_1 (or I_2), the computation along the line $\theta_\zeta = \pi$ (or $\theta_\zeta = -\pi$), which can be done independently of the surrounding data because of $\sin\theta_\zeta = 0$, is done first, and then the computation in I_1 (or I_2) is done with the aid of the data on $\hat{r} = L_2/L_1$ and $\theta_\zeta = \pi$ (or $\hat{r} = L_2/L_1$ and $\theta_\zeta = -\pi$). The computation of ($g_\#^{(n+1)}$, $h_\#^{(n+1)}$) in the domain II_1 (or II_2) is done with the aid of the data on $\hat{r} = 1$ and $\theta_\zeta = \pi/2$ (or $\hat{r} = 1$ and $\theta_\zeta = -\pi/2$). The data on $\theta_\zeta = 0$, which is the common boundary of II_1 and II_2, are computed independently of the surrounding data because of $\sin\theta_\zeta = 0$.

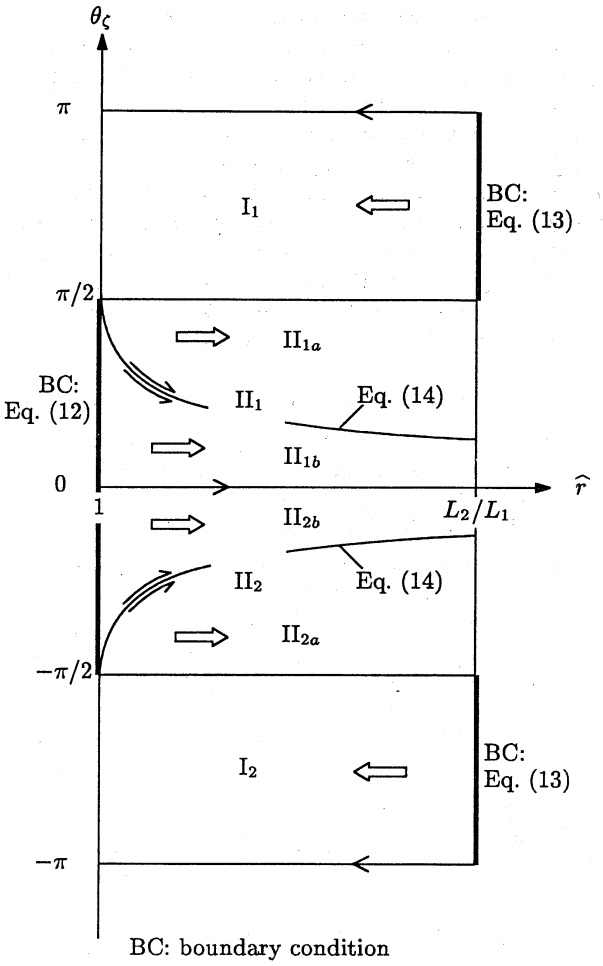

Fig. 2. Diagram of the process of computation.

(ii) On the surface of the cylinders ($\hat{r} = 1$ and L_2/L_1), the marginal velocity distribution functions g and h are discontinuous at $\theta_\zeta = \pm\pi/2$ (or $\xi_r = 0$), because the nature of the velocity distribution function of the incoming molecules and that of the outgoing molecules are different. The discontinuity propagates into the gas along the characteristic of Eq. (9) from the inner cylinder, but not from the outer cylinder, since the characteristic does not enter the gas from there.[23] Therefore, the discontinuity of (g, h) lies on the surface

$$\hat{r}\sin\theta_\zeta = 1 \qquad (-\pi/2 \le \theta_\zeta \le \pi/2). \tag{14}$$

The position of the discontinuity is independent of the molecular speed ζ. As the distance $\hat{r}$ increases, the discontinuity decays owing to molecular collisions. For small Knudsen numbers, the discontinuity from the inner cylinder is practically negligible on the outer cylinder, but for intermediate or large Knudsen numbers, it remains appreciable there.

When we discretize Eq. (9), which has the derivatives $\partial/\partial\hat{r}$ and $\partial/\partial\theta_\zeta$, we should not apply finite-difference

formulas for differentiation that contain the data across the discontinuity. Therefore, we divide the domain II_1 (or II_2) into two regions II_{1a} and II_{1b} (or , II_{2a} and II_{2b}) (Fig. 2) by discontinuity surface (14) and apply standard finite-difference approximations in each region. In this scheme, the limiting values of $(g_{\#}^{(n)}, h_{\#}^{(n)})$ on the discontinuity surface from both sides are required as the boundary condition. They are obtained separately by integration of Eq. (9) along the characteristic (14). In the region where the discontinuity has decayed sufficiently, we use a standard finite-difference scheme without dividing the domain for efficiency.

4 Free molecular and continuum solutions

In this section we explain the general behavior of the solutions of two extreme cases: the free molecular solution and the continuum solution.

4.1 Free molecular solution

The free molecular solution is easily obtained by the standard method[18,19] as follows:

$$f = \frac{\rho_{s1}}{(2\pi RT_1)^{3/2}} \exp\left(\frac{V_{\theta 1}^2}{2RT_1}\left[\left(\frac{r}{L_1}\right)^2 - 1\right]\right) \times \exp\left(-\frac{\xi_r^2 + (\xi_\theta - V_{\theta 1} r/L_1)^2 + \xi_z^2}{2RT_1}\right), \quad [\xi_r > 0 \text{ and } -L_1/r < \xi_\theta/(\xi_r^2+\xi_\theta^2)^{1/2} < L_1/r], \tag{15a}$$

$$= \frac{\rho_{s2}}{(2\pi RT_2)^{3/2}} \exp\left(-\frac{V_{\theta 2}^2}{2RT_2}\left[1 - \left(\frac{r}{L_2}\right)^2\right]\right) \times \exp\left(-\frac{\xi_r^2 + (\xi_\theta - V_{\theta 2} r/L_2)^2 + \xi_z^2}{2RT_2}\right), \quad [\text{for the other values of } \xi_r \text{ and } \xi_\theta]. \tag{15b}$$

The contributions of the two cylinders are independent. The macroscopic variables, which are obtained by moments of the distribution function, are expressed by the sum of two contributions.

The mass flow J and the energy flow W from the inner cylinder to the outer per unit time and unit length of the cylinders are

$$\begin{aligned} J &= 2\pi L_1 (m_I - m_O), \\ m_I &= \frac{p_{s1}}{(2\pi RT_1)^{1/2}}, \\ m_O &= \frac{p_{s2}}{(2\pi RT_2)^{1/2}} \exp\left(-\frac{V_{\theta 2}^2}{2RT_2}\left[1 - \left(\frac{L_1}{L_2}\right)^2\right]\right), \end{aligned} \tag{16}$$

and

$$\begin{aligned} W &= 2\pi L_1 (w_I - w_O), \\ w_I &= p_{s1}\left(\frac{RT_1}{2\pi}\right)^{1/2}\left(2 + \frac{V_{\theta 1}^2}{2RT_1}\right), \\ w_O &= p_{s2}\left(\frac{RT_2}{2\pi}\right)^{1/2}\left[2 + \frac{V_{\theta 2}^2}{2RT_2}\left(\frac{L_1}{L_2}\right)^2\right] \\ &\quad \times \exp\left(-\frac{V_{\theta 2}^2}{2RT_2}\left[1 - \left(\frac{L_1}{L_2}\right)^2\right]\right), \end{aligned} \tag{17}$$

where m_I and w_I are the contributions of the inner cylinder and m_O and w_O are those of the outer cylinder. The mass flow rate J is independent of the circumferential velocity $V_{\theta 1}$ of the inner cylinder, and increases with the speed $|V_{\theta 2}|$ of the outer cylinder.

4.2 Continuum solution

The solution of the continuum limit (Kn $\to$ 0) can be obtained by the asymptotic theory developed in Refs. 24 and 25. When evaporation or condensation is taking place on the cylinders, the behavior of the gas is described by the following system of equations and boundary conditions. The equations are the Euler set of equations:

$$\frac{d}{dr}(\rho u_r r) = 0, \tag{18}$$

$$\rho\left(u_r \frac{du_r}{dr} - \frac{u_\theta^2}{r}\right) + \frac{dp}{dr} = 0, \tag{19}$$

$$u_r \frac{du_\theta r}{dr} = 0, \tag{20}$$

$$u_r \frac{d}{dr}(u_r^2 + u_\theta^2 + 5RT) = 0, \tag{21}$$

$$p = R\rho T. \tag{22}$$

In terms of the Mach number M_r, with sign, of the radial velocity component u_r:

$$M_r = u_r/\sqrt{5RT/3}, \tag{23}$$

the boundary conditions on the cylinders are given as follows: at $r = L_1$

$$u_\theta = V_{\theta 1}, \quad p = p_{s1} h_1(M_r), \quad T = T_1 h_2(M_r), \quad (0 < M_r \le 1), \tag{24a}$$

$$p = p_{s1} F_s(-M_r, |(u_\theta - V_{\theta 1})/\sqrt{5RT/3}|, T/T_1), \quad (-1 < M_r < 0), \tag{24b}$$

$$p > p_{s1} F_b(-M_r, |(u_\theta - V_{\theta 1})/\sqrt{5RT/3}|, T/T_1), \quad (M_r \le -1), \tag{24c}$$

and at $r = L_2$

$$u_{\theta 2} = V_{\theta 2}, \quad p = p_{s2} h_1(-M_r), \quad T = T_2 h_2(-M_r), \quad (-1 \le M_r < 0), \tag{25a}$$

$$p = p_{s2} F_s(M_r, |(u_\theta - V_{\theta 2})/\sqrt{5RT/3}|, T/T_2), \quad (0 < M_r < 1), \tag{25b}$$

$$p > p_{s2} F_b(M_r, |(u_\theta - V_{\theta 2})/\sqrt{5RT/3}|, T/T_2), \quad (M_r \ge 1), \tag{25c}$$

where the functions h_1 and h_2, obtained from the solution of the half-space problem of evaporation, are listed in Refs. 24 and 26, and the function F_s and F_b, obtained from the half-space problem of condensation with a parallel flow, are shown in Ref. 27. In the flow a discontinuity (or a shock wave) is allowed, where the Rankine-Hugoniot relation should be satisfied.[28]

The general solution of the set of equations (18) – (22) (an isentropic circulating source or sink flow)[29,30] is expressed by the following parametric representation in terms of the Mach number M

$$M = \sqrt{\frac{3(u_r^2 + u_\theta^2)}{5RT}}. \tag{26}$$

That is,

$$\frac{\rho}{\rho_*} = \left(\frac{4}{3+M^2}\right)^{3/2}, \quad \frac{p}{p_*} = \left(\frac{4}{3+M^2}\right)^{5/2}, \tag{27a}$$
$$\frac{\rho}{\rho_*} = \left(\frac{4}{3+M^2}\right)^{3/2}, \quad \frac{T}{T_*} = \frac{4}{3+M^2}, \quad \rho_* = \frac{p_*}{RT_*},$$

$$M_r = M\left(\frac{3+M^2}{4}\right)^{3/2} \times \left[\sin^2\alpha_* + \left(\frac{3+M^2}{4}\right)^3 \cos^2\alpha_*\right]^{-1/2} \cos\alpha_*. \tag{27b}$$

$$\frac{r}{r_*} = \frac{1}{M}\left(\frac{3+M^2}{4}\right)^{1/2} \times \left[\sin^2\alpha_* + \left(\frac{3+M^2}{4}\right)^3 \cos^2\alpha_*\right]^{1/2}, \tag{27c}$$

$$u_r = \left(\frac{\rho_* r_*}{\rho r}\right)\left(\frac{5RT_*}{3}\right)^{1/2} \cos\alpha_*, \tag{27d}$$
$$u_\theta = \left(\frac{r_*}{r}\right)\left(\frac{5RT_*}{3}\right)^{1/2} \sin\alpha_*,$$

where p_*, T_*, r_*, and α_* are arbitrary constants. The constants ρ_*, p_*, T_*, α_*, and r_* are, respectively, the density, the pressure, the temperature, the angle of deflection of the flow velocity from the radial direction, and the radial coordinate at the hypothetical point with $M = 1$ (sonic point). In Fig. 3, the relations $|M_r|$ vs M and r/r_* vs M_r are shown for various α_*. The r/r_* takes the minimum value at $|M_r| = 1$. Thus the solution is classified into four types: $M_r \le -1$, $-1 \le M_r < 0$, $0 < M_r \le 1$, and $M_r \ge 1$. The M_r naturally varies along the flow but never exceeds the above limits in the continuous flow. A shock wave (discontinuity) is allowed in a flow with $|M_r| > 1$, where the flow can be decelerated from $|M_r| > 1$ to $|M_r| < 1$.

With the aid of the general solution, let us overview the feature of the evaporation-condensation problem. From the relation between M_r and r/r_*, the flow cannot be accelerated or decelerated across $|M_r| = 1$ (the sonic speed with respect to M_r), and from Eqs. (24a) and (25a) the evaporating speed on the condensed phase is limited by $|M_r| \le 1$. Thus, only three types of flow are possible in the present evaporation-condensation problem: (i) When evaporation is taking place on the outer cylinder ($M_r < 0$), the flow is subsonic with respect to M_r and accelerating (circulating sink flow). When the evaporation is taking place on the inner cylinder ($M_r > 0$), (ii) the flow is subsonic with respect to M_r and decelerating (circulating source flow) or (iii) the flow is an accelerating flow evaporating from the inner cylinder with $M_r = 1$ and may be accompanied by a shock wave in the middle region.

When the saturation gas pressure p_{s1} of the inner cylinder is larger than that p_{s2} of the outer cylinder ($p_{s1} > p_{s2}$), evaporation on the outer cylinder [or a flow of type (i)] is impossible. In fact, in the flow of type (i) the pressure decreases along the flow [$p(r = L_1) < p(r = L_2)$], but from the boundary conditions (24b) and (25a) with the inequalities $h_1(|M_r|) \le 1$ and $F_s \ge 1$, it follows that $p(r = L_2) < p_{s2}$ and $p(r = L_2) > p_{s1}$; the two relations contradict when $p_{s1} > p_{s2}$.

On the other hand, when $p_{s1} < p_{s2}$, the situation is complicate: evaporation on either of the cylinders is possible and bifurcation of flow is expected. For example, when both the cylinders are at rest, the gas evaporates obviously on the outer cylinder and proceeds radially to the inner cylinder without circulating motion [a flow of type (i) with $u_\theta = 0$]. If the inner cylinder begins to rotate from this state, the flow remains radial ($u_\theta = 0$) from Eq. (20) or (27d) and the boundary condition (25a) on the outer cylinder, which is at rest, but the mass flow rate decreases. The boundary condition (24b) on the inner cylinder, where condensation is tak-

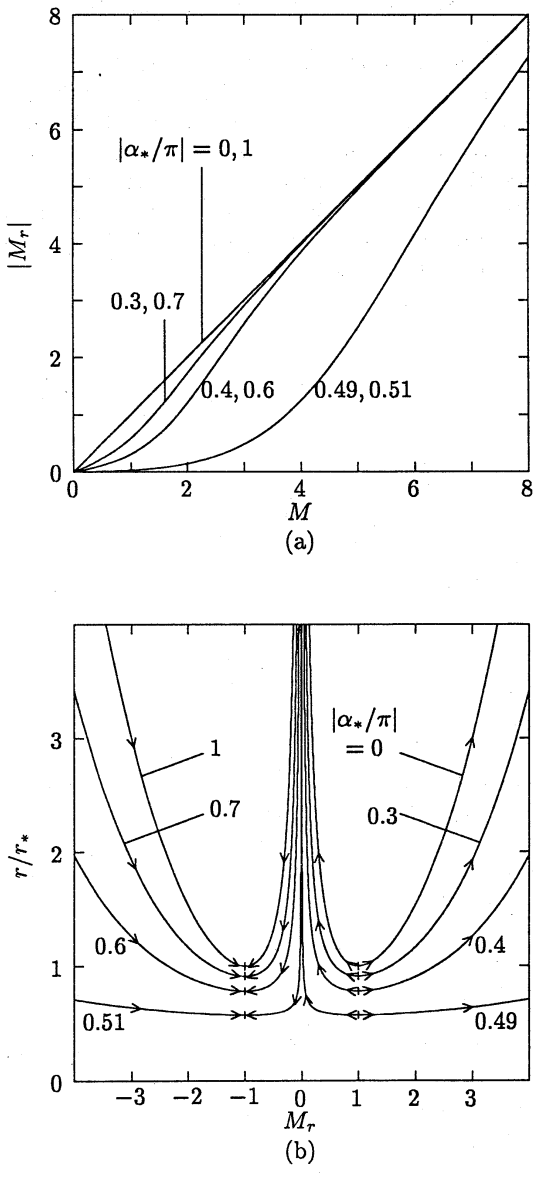

Fig. 3. Solution in the continuum limit. (a) $|M_r|$ vs M; (b) r/r_* vs M_r. The arrows on the curves in (b) indicate the direction of flow. It is found that $|M_r|$ is a monotonic increasing function of M and that r/r_* takes the minimum value at $|M_r| = 1$.

ing place, binds the pressure but not the circumferential velocity there. Next let us imagine that the system is making a solid rotation with a large angular speed. Then the pressure of the gas increases rapidly with radial distance because of the centrifugal force, and the pressure on the outer cylinder would be larger than p_{s2} and that on the inner cylinder would be smaller than p_{s1}. Thus evaporation takes place on the inner cylinder and condensation on the outer (even if $p_{s1} < p_{s2}$). Then the speed of rotation of the outer cylinder is decreased to rest. Similar flow (a circulating source flow) would be maintained, because the circumferential motion is determined by the condition of the inner cylinder and the boundary condition of the outer cylinder does not restrict the circumferential velocity u_θ. This consideration suggests the possibility of bifurcation of flow when the inner cylinder is rotating fast and the outer is at rest.

When the evaporation or condensation happens to vanish ($u_r = 0$), the set of Eqs. (18) – (22) degenerates to an undetermined system, and the higher-order analysis of the asymptotic expansion of the Boltzmann equation is required to obtain the determined system, which is derived in Ref. 25 together with its boundary condition on the cylinders (see also Ref. 31). That is, the set of equations is

$$\frac{\rho u_\theta^2}{r} - \frac{dp}{dr} = 0, \tag{28}$$

$$\Lambda\left(\frac{du_\theta}{dr} + \frac{u_\theta}{r}\right) = \frac{\gamma_1}{r}\frac{d}{dr}\left[r^2 T^m\left(\frac{du_\theta}{dr} - \frac{u_\theta}{r}\right)\right], \tag{29}$$

$$\begin{aligned}\Lambda\frac{d}{dr}\left(\frac{u_\theta^2}{2} + \frac{5RT}{2}\right) &= \gamma_1\frac{d}{dr}\left[rT^m u_\theta\left(\frac{du_\theta}{dr} - \frac{u_\theta}{r}\right)\right] \\ &+ \frac{5\gamma_2 R}{2}\frac{d}{dr}\left[rT^m\frac{dT}{dr}\right],\end{aligned} \tag{30}$$

$$p = R\rho T, \tag{31}$$

where $m = 1/2, \gamma_1 = 1.270042, \gamma_2 = 1.922284$ for a hard-sphere molecular gas, $m = 1, \gamma_1 = 1, \gamma_2 = 1$ for the BKW equation, and Λ is a constant to be determined with the solution (u_θ, ρ, p, T). The physical meaning of Λ is as follows: If the rarefaction of the gas (or the effect of the mean free path of the gas molecules) were taken into account, the radial velocity u_r would not be zero. Then,

$$\Lambda = c_0 u_r r T^m (RT)^{-1/2} l^{-1}, \tag{32}$$

where l is the local mean free path of the gas molecules and c_0 is a nondimensional constant [$c_0 = 2\sqrt{2/\pi}$ (hard-sphere and BKW)]. The set of equations (28)–(32) is equivalent to the set of the axially and circumferentially uniform Navier-Stokes equations where the radial velocity of the order of the Knudsen number is retained. The boundary conditions for the set of equations on the two cylinders are

$$\begin{aligned} u_\theta &= V_{\theta 1}, \quad T = T_1, \quad p = p_{s1} \quad (\text{at } r = L_1), \\ u_\theta &= V_{\theta 2}, \quad T = T_2, \quad p = p_{s2} \quad (\text{at } r = L_2). \end{aligned} \tag{33}$$

The system of equations (28) – (31) and boundary conditions (33) is a determined system, where the set of one

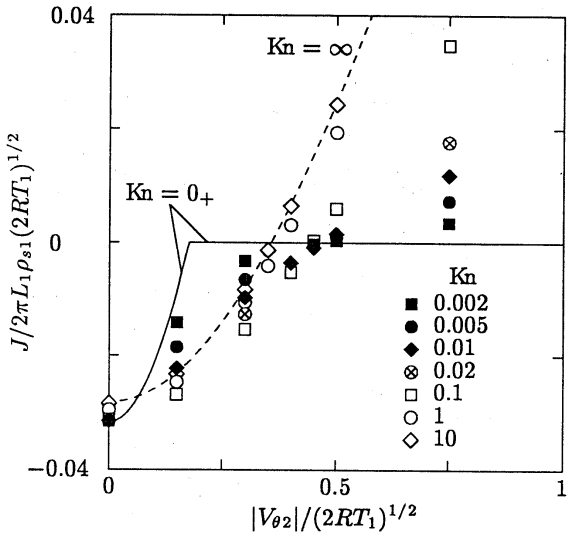

Fig. 4. The mass-flow rate J versus the circumferential speed $|V_{\theta 2}|$ of the outer cylinder ($L_2/L_1 = 2$, $p_{s2}/p_{s1} = 1.1$, $T_2/T_1 = 1$, and $V_{\theta 1} = 0$). The numerical solutions of the BKW equation for various Kn are shown by the symbols: ■: Kn=0.002; ●: 0.005; ♦: 0.01; ⊗: 0.02; □: 0.1; ○: 1; ◇: 10. The solid line ——: the solution at Kn= 0_+ by the asymptotic analysis in Sec. 4.2. The dashed line - - - - : the free molecular solution.

algebraic equation and one first-order and two second-order differential equations for four functions (u_θ, ρ, p, T) with an undetermined constant (Λ) is to be obtained under six boundary conditions. It is noted that the behavior of the gas at Kn = 0_+ is determined together with a quantity of the order of Kn (or u_r). That is, it is not the conventional cylindrical Couette flow [the axially and circumferentially uniform solution of the Navier-Stokes equation under the nonslip boundary condition without evaporation-condensation ($u_r = 0$) on the boundary] except when $\Lambda = 0$.

In the next section we will discuss the flow in the whole range of the Knudsen number (including the more explicit description of the two limiting solutions) for $p_{s2} > p_{s1}$, where bifurcation and reversal of a flow are expected.

5 Flows in the whole range of the Knudsen number and discussions

5.1 Reversal of flow

First, we consider the case where the inner cylinder is at rest [$V_{\theta 1}/(2RT_1)^{1/2} = 0$]. Taking $p_{s2}/p_{s1} = 1.1$, $T_2/T_1 = 1$, and $L_2/L_1 = 2$, we investigate the behavior of the gas numerically for various values of the parameters Kn and $V_{\theta 2}/(2RT_1)^{1/2}$. The temperature ratio is put equal to unity by the reason explained in the last paragraph of Sec. 2. The results of computation together with those for the free molecular and continuum flows are given in Figs. 4–9, on the basis of which we will discuss the feature of the flow.

In order to grasp the overall feature of the flow in the domain of the parameters Kn and $V_{\theta 2}/(2RT_1)^{1/2}$, we first discuss the mass-flow rate between the cylinders.

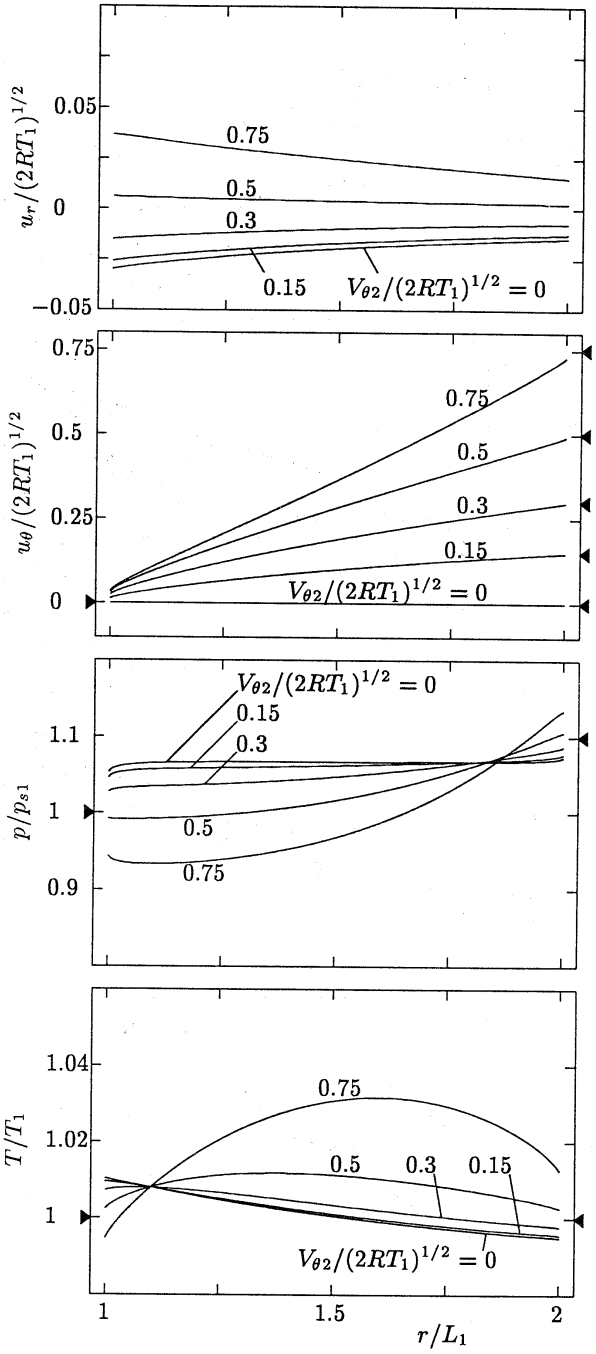

Fig. 5. The profiles of the flow velocity (u_r, u_θ), pressure p, and temperature T of the gas for various circumferential velocities $V_{\theta 2}$ of the outer cylinder when the inner cylinder is at rest I: (Kn= 0.1, $p_{s2}/p_{s1} = 1.1$, $T_2/T_1 = 1$, $L_2/L_1 = 2$). The symbol ▶ (◀) indicates the position corresponding to $V_{\theta 1}$, p_{s1}, or T_1 ($V_{\theta 2}$, p_{s2}, or T_2).

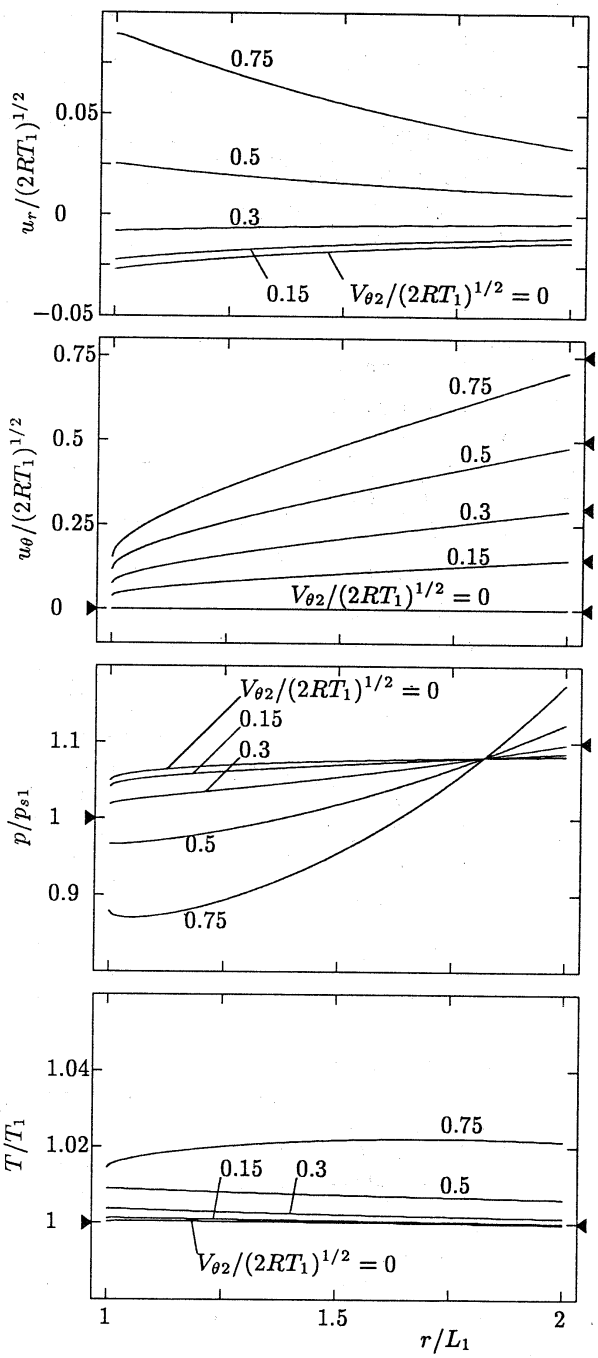

Fig. 6. The profiles of the flow velocity (u_r, u_θ), pressure p, and temperature T of the gas for various circumferential velocities $V_{\theta 2}$ of the outer cylinder when the inner cylinder is at rest II: (Kn= 10, $p_{s2}/p_{s1} = 1.1$, $T_2/T_1 = 1$, $L_2/L_1 = 2$). The symbol ▶ (◀) indicates the position corresponding to $V_{\theta 1}$, p_{s1}, or T_1 ($V_{\theta 2}$, p_{s2}, or T_2).

The mass-flow rate J from the inner to outer cylinder versus the speed $V_{\theta 2}$ of the outer cylinder is shown for various Knudsen numbers from Kn = 0 to ∞ in Fig. 4.

In the free molecular flow, as explained in Sec. 4.1, the effects of the inner and outer cylinders are independent of each other. All the molecules leaving the inner cylinder reach the outer cylinder. On the other hand, some molecules leaving the outer cylinder do not reach the inner cylinder and return directly to some other point on the outer cylinder. This is determined by the direction of the velocity of a molecule leaving the inner cylinder. As the speed of the outer cylinder increases, the number of molecules that reach the inner cylinder decreases and finally no molecules reach it,

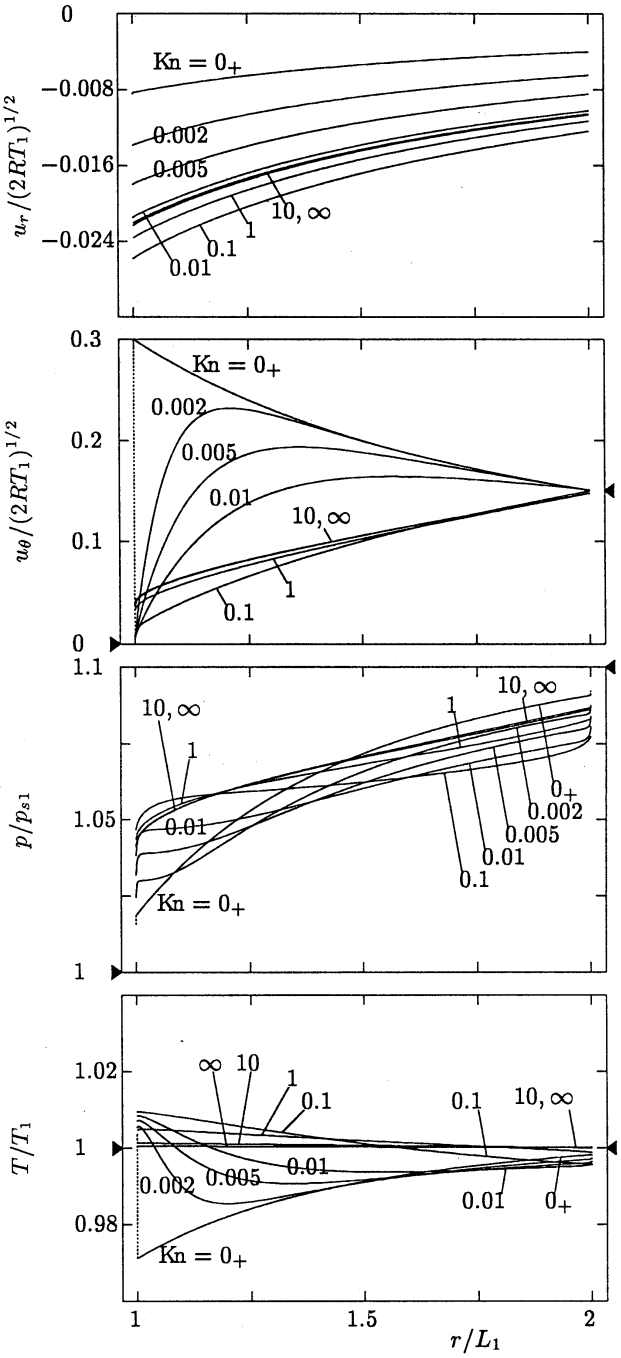

Fig. 7. The profiles of the flow velocity (u_r, u_θ), pressure p, and temperature T of the gas for various Knudsen numbers Kn when the inner cylinder is at rest I: $(V_{\theta 2}/(2RT_1)^{1/2} = 0.15$, $p_{s2}/p_{s1} = 1.1$, $T_2/T_1 = 1$, $L_2/L_1 = 2)$. The dotted line ····· indicates the Knudsen layer flattened on the cylinders at Kn= 0_+. The symbol ▶ (◀) indicates the position corresponding to $V_{\theta 1}$, p_{s1}, or T_1 ($V_{\theta 2}$, p_{s2}, or T_2).

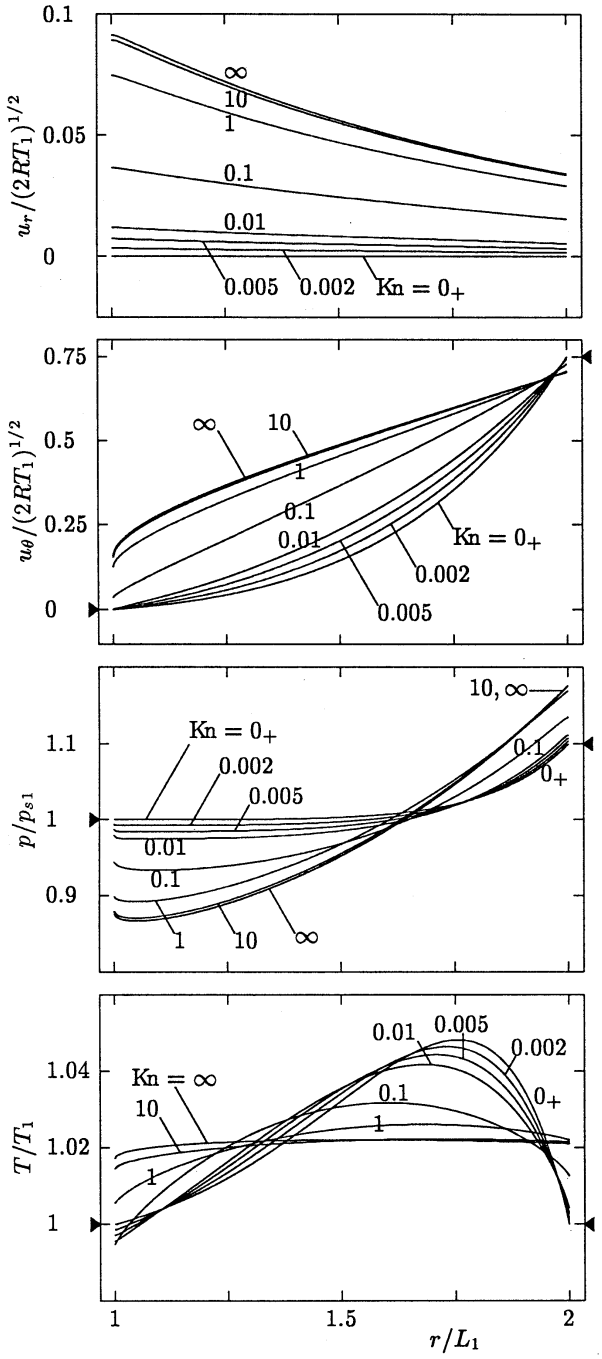

Fig. 8. The profiles of the flow velocity (u_r, u_θ), pressure p, and temperature T of the gas for various Knudsen numbers Kn when the inner cylinder is at rest II: $[V_{\theta 2}/(2RT_1)^{1/2} = 0.75$, $p_{s2}/p_{s1} = 1.1$, $T_2/T_1 = 1$, $L_2/L_1 = 2]$. The symbol ▶ (◀) indicates the position corresponding to $V_{\theta 1}$, p_{s1}, or T_1 ($V_{\theta 2}$, p_{s2}, or T_2).

since the high speed motion of the outer cylinder imparts a large circumferential motion to the molecules leaving the outer cylinder. Thus, the net mass-flow rate (from the inner cylinder to the outer) increases from $2\pi L_1(2\pi RT_1)^{-1/2}[p_{s1} - p_{s2}(T_1/T_2)^{1/2}]$ to $2\pi L_1 p_{s1}$ $(2\pi RT_1)^{-1/2}$ (or a negative to a positive value). That is, evaporation takes place on the outer cylinder and condensation on the inner when both the cylinders are at rest. As the speed of the outer cylinder increases, the rate of evaporation on the outer cylinder decreases and vanishes at some speed, and then reversal of the flow or evaporation on the inner cylinder occurs.

In the continuum flow (Kn = 0_+), as in the free molecular flow, evaporation takes place on the outer cylinder and condensation on the inner when both the cylinders are at rest, and as the speed of the outer cylinder increases, the rate of evaporation on the outer cylinder decreases and vanishes at the speed

$$|V_{\theta 2}| = \frac{(5RT_2)^{1/2}[1-(p_{s2}/p_{s1})^{-2/5}]^{1/2}}{[(L_2/L_1)^2-1]^{1/2}} = 0.1766(2RT_1)^{1/2}. \quad (34)$$

(This result is independent of molecular models. The first formula applies to arbitrary values of p_{s2}/p_{s1}, T_2/T_1, and L_2/L_1.) For the higher speed of the outer cylinder, in contrast to the free molecular flow, no reversal of flow takes place, and neither evaporation nor condensation occurs on the cylinders, because evaporation on the inner cylinder at rest does not supply circumferential motion. The solution without evaporation and condensation is obtained by the system (28)–(31) and (33). According to Λ, determined by these equations, the Kn-order term of the nondimensional mass-flow rate $J/2\pi L_1\rho_{s1}(2RT_1)^{1/2}$ is negative for $|V_{\theta 1}|/(2RT_1)^{1/2} < 0.4697$ and positive for $|V_{\theta 1}|/(2RT_1)^{1/2} > 0.4697$. (This value is 0.4693 for a hard-sphere molecular gas.) Correspondingly, the profiles of the flow field at Kn $=0_+$ is different from that of the conventional Couette flow (the solution of the Navier-Stokes equation with $u_r = 0$) except at $|V_{\theta 1}|/(2RT_1)^{1/2} = 0.4697$. This is studied in detail in Refs. 25 as an example showing the incompleteness of the classical gas dynamics.[32]

The mass-flow rate in the intermediate Knudsen numbers increases monotonically with the speed $|V_{\theta 2}|$ of the outer cylinder. The variation of the mass-flow rate with the Knudsen number is not monotonic when $|V_{\theta 2}|$ is smaller than about $\sqrt{RT_1/2}$. This is discussed in relation to the profile of flow field later.

The profiles of the velocity, pressure, and temperature at Kn = 0.1 and 10 are shown for various speeds of the outer cylinder in Figs. 5 and 6, where we can see the variation of the flow field with the speed of the outer cylinder. The circumferential motion of the outer cylinder is transmitted to the whole region of the gas, inducing pressure variation owing to the centrifugal force. As the speed of the outer cylinder increases, the pressure near the outer cylinder exceeds p_{s2} and the pressure near the inner cylinder goes down below p_{s1}. This results in the reversal of the flow (from $u_r < 0$ to $u_r > 0$). The qualitative feature is the same for both the Knudsen numbers. The temperature field at Kn= 0.1 clearly shows the combination of the heating effect of gas motion and temperature jump (or drop) on the condensing (evaporating) boundary. The heating is obviously stronger for faster motion, and the jump (or drop) is bigger for stronger condensation (or evaporation). The latter contribution is not so evident at Kn= 10.

Figures 7 and 8 show the profiles for various Knudsen numbers at $|V_{\theta 2}|/(2RT_1)^{1/2} = 0.15$ and 0.75. In these figures we can see the variation of the flow field with the Knudsen number.

In the case of $|V_{\theta 2}|/(2RT_1)^{1/2} = 0.15$ (fairly small $|V_{\theta 2}|$, Fig. 7), the circumferential velocity at Kn = 0_+,

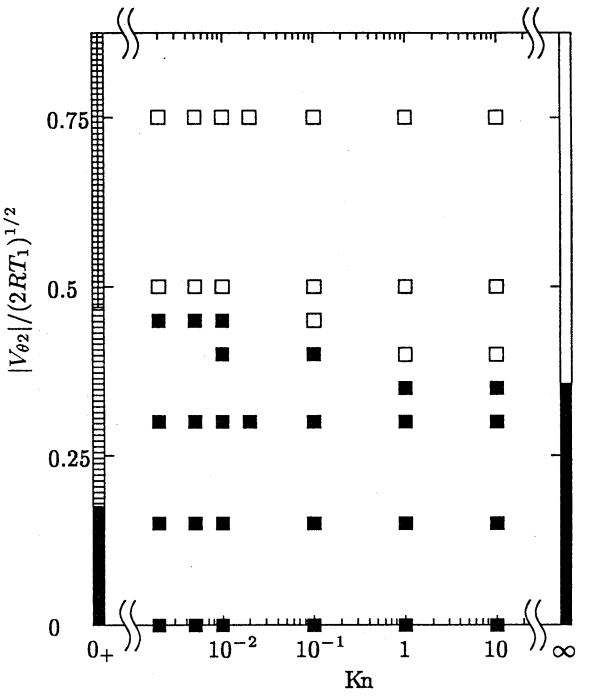

Fig. 9. The type of solutions classified by the direction of flow in the plane (Kn, $V_{\theta 2}/(2RT_1)^{1/2}$) for $L_2/L_1 = 2$, $p_{s2}/p_{s1} = 1.1$, $T_2/T_1 = 1$, and $V_{\theta 2} = 0$. The type of a solution is indicated by the symbols: □ (point) and ▭ (range): a solution with $u_r > 0$; ■ (point) and ▬ (range): $u_r < 0$; ▦ at Kn = 0_+: $u_r = O(\mathrm{Kn}) > 0$; ▥ at Kn = 0_+: $u_r = O(\mathrm{Kn}) < 0$.

where the flow is isentropic and evaporation is taking place on the outer cylinder, is determined by the velocity $V_{\theta 2}$ of the outer cylinder and is not affected by the velocity $V_{\theta 1}$ of the inner cylinder. As the Knudsen number increases, the effect of the stationary inner cylinder is transmitted into the gas and the circumferential motion of the gas is retarded. This reduces the pressure near the outer cylinder and increases the pressure near the inner cylinder. Thus the rate of evaporation on the outer cylinder increases. This increase ceases at about Kn = 0.1; then it decreases to the value at Kn = ∞ (see also Fig. 4). This maximum is the result of different dependence on the Knudsen number for large and small Kn, as in the Knudsen minimum in the Poiseuille flow of a rarefied gas.[19,33] This behavior for large Knudsen numbers can be understood in the following way. At Kn = ∞, all the molecules from the inner cylinder reach the outer directly. At a large but not infinite Kn, molecular collisions block some of the molecules to reach the outer cylinder; in return the molecules from the outer cylinder are subject to collision effect, but only a part of them was to reach the inner cylinder without collisions. Thus the latter blocking effect is smaller than the former. The number of molecules from the outer to the inner cylinder, therefore, is bigger with molecular collision. This nonmonotonic dependence on Kn is seen for $0 < |V_{\theta 2}|/(2RT_1)^{1/2} \lesssim 0.45$.

In the case $|V_{\theta 2}|/(2RT_1)^{1/2} = 0.75$ (Fig. 8), neither evaporation nor condensation occurs on the cylinders

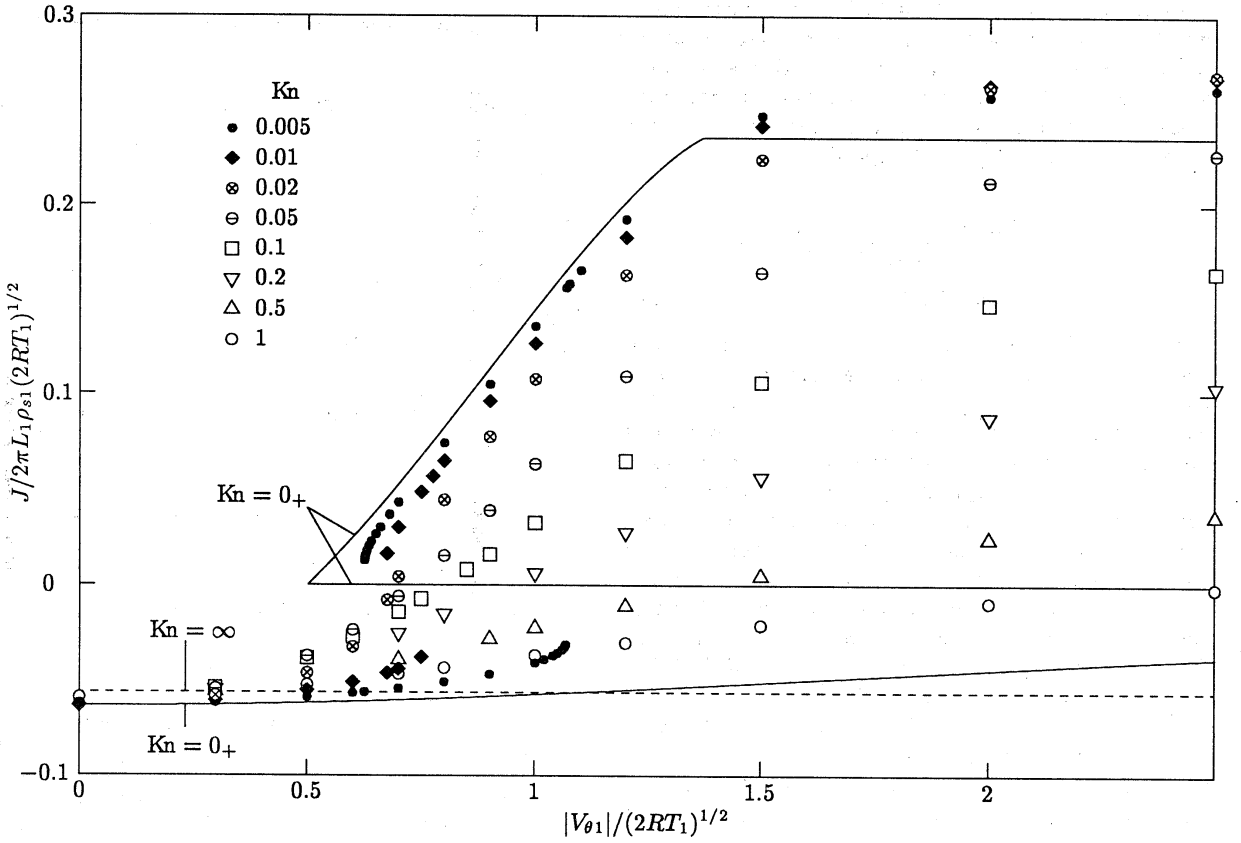

Fig. 10. The mass-flow rate J versus the circumferential speed $|V_{\theta 1}|$ of the inner cylinder ($L_2/L_1 = 2$, $p_{s2}/p_{s1} = 1.2$, $T_2/T_1 = 1$, and $V_{\theta 2} = 0$). The numerical solutions of the BKW equation for various Kn are shown by the symbols: ●: Kn = 0.005; ◆: 0.01; ⊗: 0.02; ⊖: 0.05; □: 0.1; ▽: 0.2; △: 0.5; ○: 1. The solid line ——: the solution at Kn= 0_+ by the asymptotic analysis in Sec. 4.2. The dashed line - - - - - : the free molecular solution.

at Kn= 0_+. As already mentioned, the profiles, obtained by Eqs. (28)–(31) and (33), are different from those of the conventional cylindrical Couette flow. At this value of $|V_{\theta 2}|/(2RT_1)^{1/2}$, Λ is positive, that is, the radial velocity u_r of the order Kn is positive. As the Knudsen number increases, the effect of the circumferential motion of the outer cylinder is further transmitted into the gas for small Kn and induces higher pressure near the outer cylinder owing to the additional centrifugal force, or the blocking effect of molecular collisions, discussed in the case of $|V_{\theta 2}|/(2RT_1)^{1/2} = 0.15$, decreases for large Kn. Thus, in contrast to the case of $|V_{\theta 2}|/(2RT_1)^{1/2} = 0.15$, the flow to the outer cylinder increases monotonically with Kn.

As the summary of this subsection, the type of solutions classified by the direction of flow ($u_r > 0$ or $u_r < 0$) is shown on the parameter plane (Kn, $|V_{\theta 2}|/(2RT_1)^{1/2}$) in Fig. 9. At Kn= 0_+, the evaporation-condensation ceases for $|V_{\theta 2}|/(2RT_1)^{1/2} \geq 0.1766$; the sign of u_r of the order of Kn in this range of $|V_{\theta 2}|/(2RT_1)^{1/2}$, which is obtained by asymptotic analysis of the BKW equation, is also shown. Only one solution exits for a set of (Kn, $|V_{\theta 2}|/(2RT_1)^{1/2}$), and bifurcation of flow does not occur. Except for the continuum limit, reversal of flow occurs at some speed of the outer cylinder.

5.2 Bifurcation of flow

In this section we consider the case where the outer cylinder is at rest [$V_{\theta 2}/(2RT_1)^{1/2} = 0$]. Taking $p_{s2}/p_{s1} = 1.2$, $T_2/T_1 = 1$, and $L_2/L_1 = 2$, we investigate the behavior of the gas numerically for various values of the parameters Kn and $V_{\theta 1}/(2RT_1)^{1/2}$. The temperature ratio is put equal to unity by the reason explained in the last paragraph of Sec. 2. The results of computation together with those for the free molecular and continuum flows are given in Figs. 10–16, on the basis of which we will discuss the feature of the flow.

The mass-flow rate J from the inner to outer cylinder versus the speed $|V_{\theta 1}|$ of the inner cylinder is shown for various Knudsen numbers from Kn = 0 to ∞ in Fig. 10.

In the free molecular flow, where all the molecules leaving the inner cylinder reach the outer cylinder, the number of molecules leaving the inner cylinder is independent of the velocity of the inner cylinder. Thus the mass-flow rate is $2\pi L_1 p_{s1}\ (2\pi RT_1)^{-1/2}\ [1 - (p_{s2}/p_{s1})\ (T_1/T_2)^{1/2}]$ irrespective of $V_{\theta 1}$.

In the continuum flow (Kn = 0_+), on the other hand, the situation is complicate. When both the cylinders are at rest, evaporation takes place on the outer cylinder. It decreases gradually with the speed of the inner cylinder, but never vanishes until the speed becomes infinite. Besides this solution, there are two other solutions when the speed of the inner cylinder exceeds the

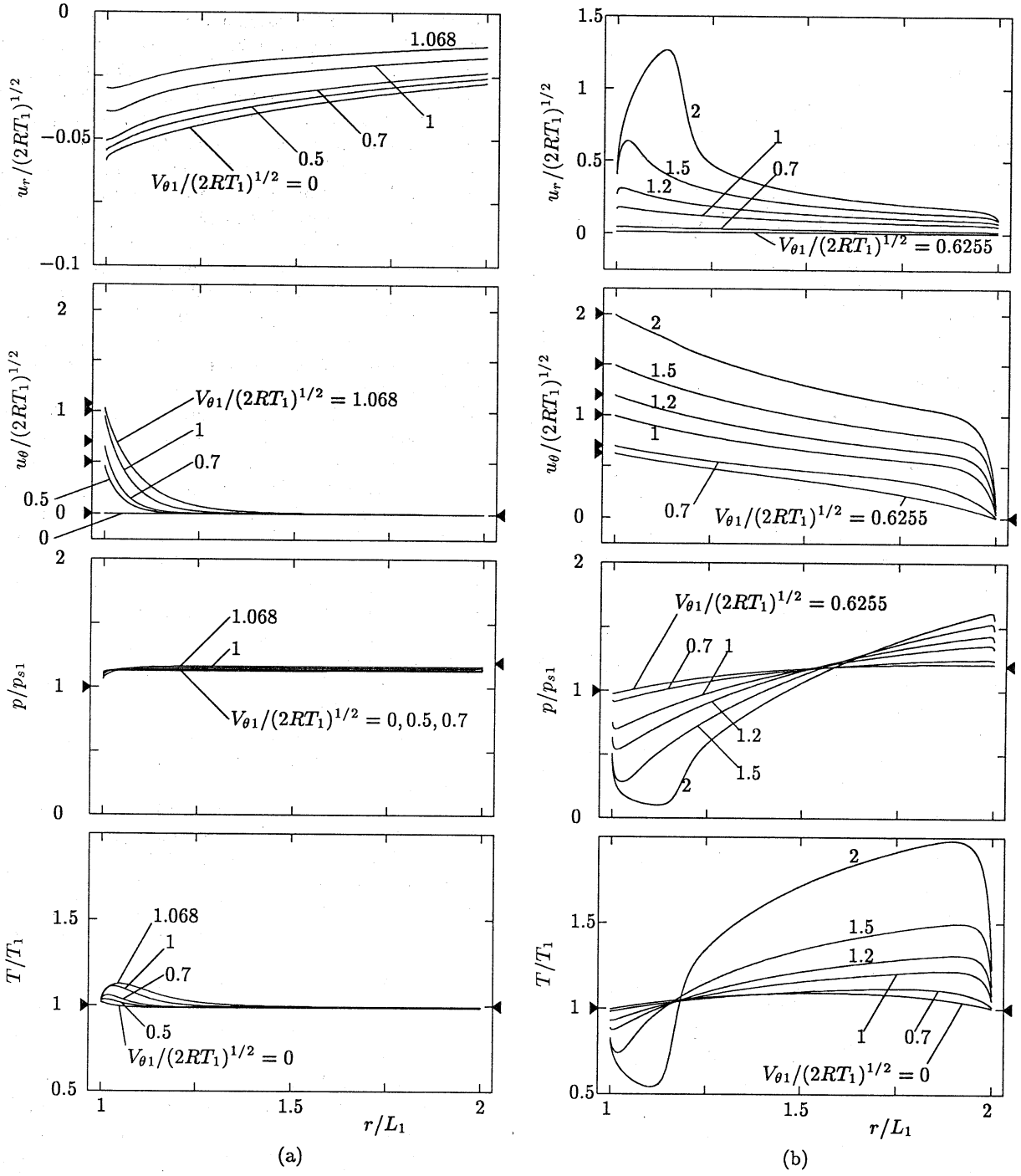

Fig. 11. The profiles of the flow velocity (u_r, u_θ), pressure p, and temperature T of the gas for various circumferential velocities $V_{\theta 1}$ of the inner cylinder when the outer cylinder is at rest I: (Kn= 0.005, $p_{s2}/p_{s1} = 1.2$, $T_2/T_1 = 1$, $L_2/L_1 = 2$). (a) The family of solutions with $J < 0$; (b) The family of solutions with $J > 0$. The symbol ▶ (◀) indicates the position corresponding to $V_{\theta 1}$, p_{s1}, or T_1 ($V_{\theta 2}$, p_{s2}, or T_2).

value

$$|V_{\theta 1}| = \frac{(5RT_1)^{1/2}[(p_{s2}/p_{s1})^{2/5} - 1]^{1/2}}{[1 - (L_1/L_2)^2]^{1/2}} = 0.5022(2RT_1)^{1/2}. \quad (35)$$

(The bifurcation of flow occurs at this speed of the inner cylinder, which is independent of molecular models. The first formula applies to arbitrary values of p_{s2}/p_{s1}, T_2/T_1, and L_2/L_1.) One of them is a flow with evaporation on the inner cylinder. The rate of evaporation J increases from zero to $0.2360(2\pi L_1)\rho_{s1}(2RT_1)^{1/2}$ as the speed $|V_{\theta 1}|$ of the inner cylinder increases from $0.5022(2RT_1)^{1/2}$ to $1.373(2RT_1)^{1/2}$, and it remains constant for the larger $|V_{\theta 1}|$. As $|V_{\theta 1}|$ increases, the speed of evaporation (or M_r) on the inner cylinder increases and reaches $M_r = 1$. Thus for the larger $|V_{\theta 1}|$, the rate

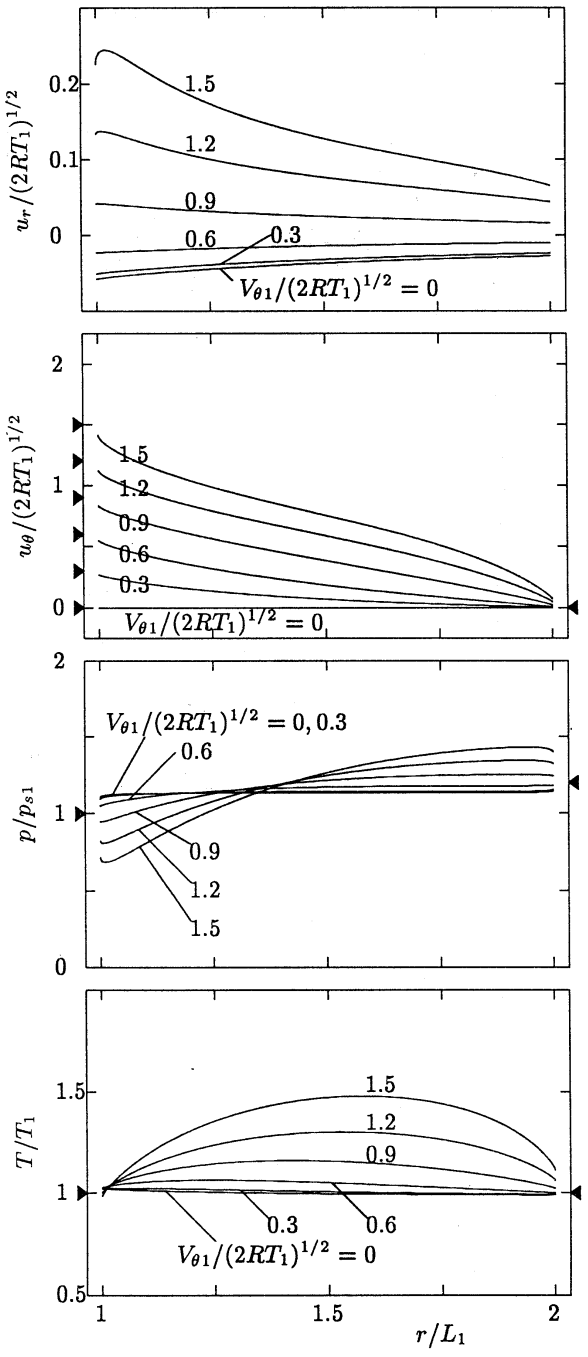

Fig. 12. The profiles of the flow velocity (u_r, u_θ), pressure p, and temperature T of the gas for various circumferential velocities $V_{\theta 1}$ of the inner cylinder when the outer cylinder is at rest II: (Kn= 0.05, $p_{s2}/p_{s1} = 1.2$, $T_2/T_1 = 1$, $L_2/L_1 = 2$). The symbol ▶ (◀) indicates the position corresponding to $V_{\theta 1}$, p_{s1}, or T_1 ($V_{\theta 2}$, p_{s2}, or T_2).

of evaporation remains constant, since evaporation with $M_r > 1$ is impossible [see Eq. (24a)]. The flow is an accelerating supersonic flow accompanied by a shock wave (Fig. 14). The other one is a flow without evaporation and condensation on the cylinders, the solution of which is obtained by the system (28)–(31) and (33). According to Λ, determined by these equations, the Kn-order term of the nondimensional mass-flow rate $J/2\ \pi L_1\ \rho_{s1}(2RT_1)^{1/2}$ is negative for $|V_{\theta 1}|/(2RT_1)^{1/2} < 0.6672$ and positive for $|V_{\theta 1}|/(2RT_1)^{1/2} > 0.6672$. (This value is 0.6593 for a hard-sphere molecular gas.) Correspondingly, the profiles of the flow field at Kn = 0_+ is different from that of the conventional Couette flow except at $|V_{\theta 1}|/(2RT_1)^{1/2} = 0.6672$. This is also an example showing the incompleteness of the classical gas dynamics discussed in Refs. 25 and 32.

The mass flow rate increases monotonically with the speed $|V_{\theta 1}|$ of the inner cylinder when the Knudsen number Kn is larger than about 0.02. For smaller Knudsen numbers the situation is quite different. There are two branches of solutions for a given Knudsen number: one is a family of flows with evaporation on the outer cylinder existing in the range $0 \le |V_{\theta 1}| \le V_A$, the rate of evaporation of which slowly decreases with $|V_{\theta 1}|$, and the other is a family of flows with condensation on the outer cylinder existing in the range $|V_{\theta 1}| \ge V_B$, the rate of condensation of which increases with $|V_{\theta 1}|$. Here, V_A and V_B depend on Kn, and $V_A > V_B$. There are two solutions in the range $V_B \le |V_{\theta 1}| \le V_A$ (bifurcation of flow). There should be the third family of solutions, corresponding to the solution with $u_r = 0$ at Kn = 0_+, that connects the two families from V_A to V_B, but it could not be obtained numerically, probably because of instability of the solution.

The profiles of the velocity, pressure, and temperature at Kn = 0.005 and 0.05 are shown for various speeds of the inner cylinder in Figs. 11 and 12, where we can see the variation of the flow field with the speed of the inner cylinder.

At Kn = 0.005, there are two families of profiles: one exists in $0 \le |V_{\theta 1}|/(2RT_1)^{1/2} \lesssim 1.068$ [Fig. 11 (a)]; the other in $|V_{\theta 1}|/(2RT_1)^{1/2} \gtrsim 0.6255$ [Fig. 11 (b)], in each of which the profiles vary smoothly with $|V_{\theta 1}|$. Two profiles are possible for $0.6255 \lesssim |V_{\theta 1}|/(2RT_1)^{1/2} \lesssim 1.068$. At $|V_{\theta 1}| = 0$, the flow is radial from the outer cylinder to the inner. As $|V_{\theta 1}|$ increases, the circumferential motion of the inner cylinder is transmitted into the gas, but its penetration is strongly blocked by the convection radial flow and reaches only half way from the inner cylinder even at $|V_{\theta 1}| = (2RT_1)^{1/2}$ (a little higher than sonic speed). Owing to this limited angular motion resulting in only small pressure rise by centrifugal force, the pressure near the outer cylinder is lower than p_{s2}, and the gas remains evaporating from the outer cylinder. For $|V_{\theta 1}|/(2RT_1)^{1/2} \gtrsim 1.075$, this type of flow no longer exists, and completely different flows appear. The angular motion comparable to that of the inner cylinder prevails over the whole field, except in a thin layer near the outer cylinder, inducing a pressure higher than p_{s2} near the outer cylinder, and therefore evaporation occurs on the inner cylinder. This type of flow exists not only for $|V_{\theta 1}|/(2RT_1)^{1/2} \gtrsim 1.075$ but also for smaller $|V_{\theta 1}|/(2RT_1)^{1/2}$ down to about 0.6255 . It was impossible to obtain a family of solutions that connects the two branches smoothly, probably because of instability of the flow.

At Kn = 0.05 (Fig. 12), the variation is smooth for all $|V_{\theta 1}|/(2RT_1)^{1/2}$; only one profile is possible for a given $|V_{\theta 1}|/(2RT_1)^{1/2}$.

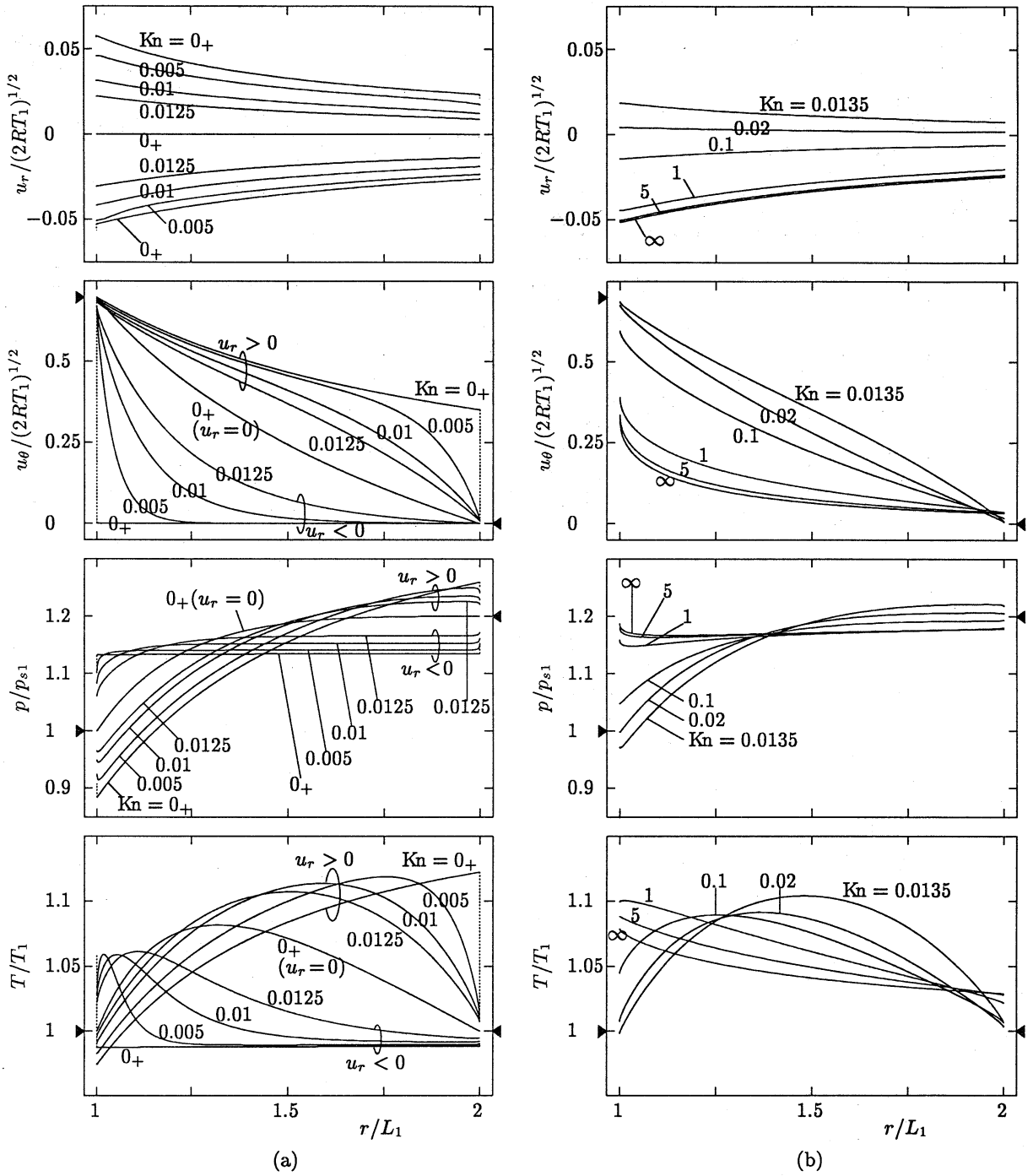

Fig. 13. The profiles of the flow velocity (u_r, u_θ), pressure p, and temperature T of the gas for various Knudsen numbers Kn when the outer cylinder is at rest I: $[V_{\theta 1}/(2RT_1)^{1/2} = 0.7$, $p_{s2}/p_{s1} = 1.2$, $T_2/T_1 = 1$, $L_2/L_1 = 2]$. (a) The profiles for Kn= 0 – 0.0125.; (b) The profiles for Kn= 0.0135 – ∞. The dotted line ····· indicates the Knudsen layer flattened on the cylinders at Kn= 0_+. The symbol ▶ (◀) indicates the position corresponding to $V_{\theta 1}$, p_{s1}, or T_1 ($V_{\theta 2}$, p_{s2}, or T_2).

Figures 13–15 show the profiles for various Knudsen numbers at $|V_{\theta 1}|/(2RT_1)^{1/2} = 0.7$, 2.5, and 0.3. In these figures, we can see the variation of the flow field with the Knudsen number.

At $|V_{\theta 1}|/(2RT_1)^{1/2} = 0.7$ (Fig. 13), there are two families of the profiles, one with $u_r < 0$ and the other with $u_r > 0$, for small Knudsen numbers (Kn is smaller than about 0.0125). (There is another solution with $u_r = 0$ at Kn = 0_+.) This nonuniqueness can be understood in the following way. Owing to the convection of the radial gas flow, the effect of circumferential motion of a condensing cylinder (the inner or outer cylinder depending on $u_r < 0$ or $u_r > 0$) on the circumferential motion of the gas hardly penetrates deep into the gas when the Knudsen number is small. Let $u_r < 0$. The flow is radial, and the circumferential motion is confined in a narrow region near the inner cylinder; thus the pressure is nearly uniform outside the region and

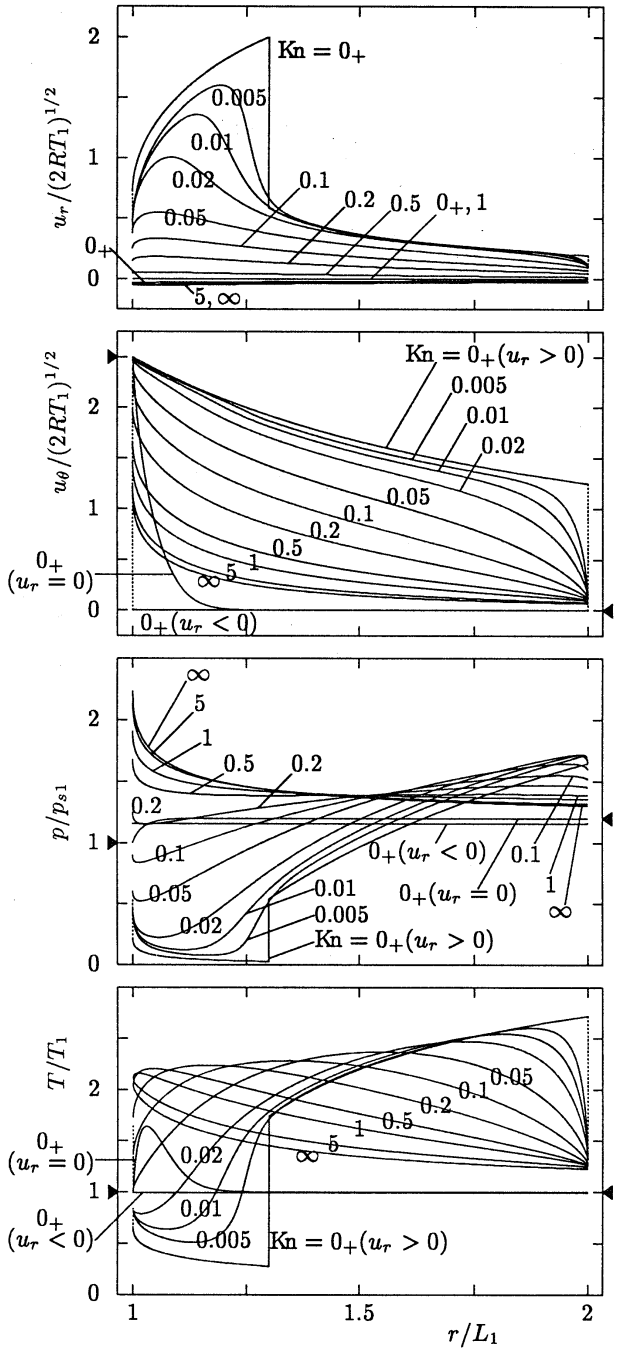

Fig. 14. The profiles of the flow velocity (u_r, u_θ), pressure p, and temperature T of the gas for various Knudsen numbers Kn when the outer cylinder is at rest II: $[V_{\theta 1}/(2RT_1)^{1/2} = 2.5$, $p_{s2}/p_{s1} = 1.2$, $T_2/T_1 = 1$, $L_2/L_1 = 2]$. The dotted line ····· indicates the Knudsen layer flattened on the cylinders at Kn= 0_+. The symbol ▶ (◀) indicates the position corresponding to $V_{\theta 1}$, p_{s1}, or T_1 ($V_{\theta 2}$, p_{s2}, or T_2).

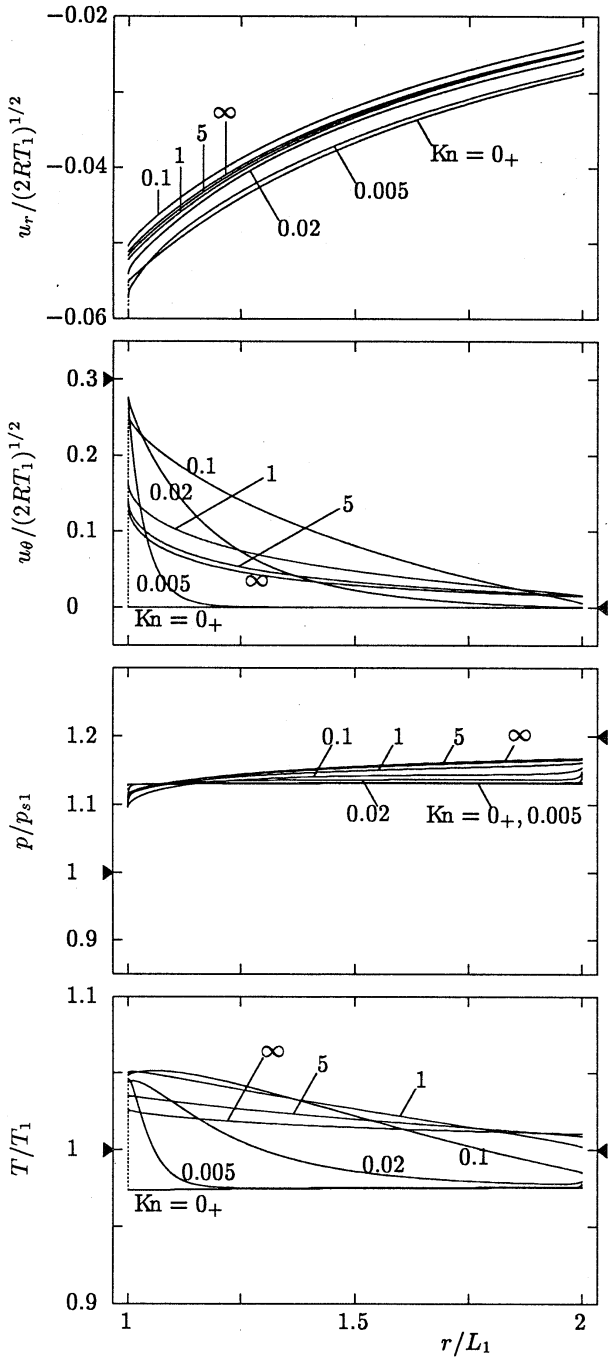

Fig. 15. The profiles of the flow velocity (u_r, u_θ), pressure p, and temperature T of the gas for various Knudsen numbers Kn when the outer cylinder is at rest III: $[V_{\theta 1}/(2RT_1)^{1/2} = 0.3$, $p_{s2}/p_{s1} = 1.2$, $T_2/T_1 = 1$, $L_2/L_1 = 2]$. The dotted line ····· indicates the Knudsen layer flattened on the cylinders at Kn= 0_+. The symbol ▶ (◀) indicates the position corresponding to $V_{\theta 1}$, p_{s1}, or T_1 ($V_{\theta 2}$, p_{s2}, or T_2).

the pressure near the outer cylinder is lower than p_{s2}. Thus in conformity with the assumption, evaporation takes place on the outer cylinder. Let $u_r > 0$. The flow is circulating over the whole field except near the outer cylinder, and a considerable pressure variation due to centrifugal force is induced and the pressure near the outer cylinder is higher than p_{s2}. Thus, in conformity with the assumption, condensation (evaporation) takes place on the outer (inner) cylinder. As the Knudsen number increases, the effect of the condensing cylinder on the circumferential motion penetrates deeper into the gas, and two solutions approach. One of the solutions ($J < 0$), however, disappears at about Kn =

0.0135, and the other solution loses its radial motion and finally reverses its direction.

At larger speed [$|V_{\theta 1}|/(2RT_1)^{1/2} = 2.5$] of the inner cylinder (Fig. 14), nonunique situation of the solution is similar to that in the previous example. The larger circumferential velocity induces the larger pressure variation to reverse the direction of flow even when the penetration of circumferential motion is not deep, and the first type flow (a flow evaporating on the outer cylinder) occurs for only smaller Knudsen numbers. Among Knudsen numbers for which the computation is carried out, only the case Kn = 0_+ is the first type of flow. Along the second type flow, the flow is first accelerated and then decelerated. The deceleration becomes sharper as the Knudsen number decreases; and finally at Kn = 0_+, the decelerated region is reduced to a discontinuity (a shock wave) accompanied by a moderately decelerating region.

At small speed [$|V_{\theta 1}|/(2RT_1)^{1/2} = 0.3$] of the inner cylinder (Fig. 15), where the solution with $u_r = 0$ at Kn = 0_+ does not exist, the pressure variation induced by circumferential motion is too small to reverse the direction of flow even if the circumferential motion is induced over the whole field, and thus evaporation takes place on the outer cylinder for all Knudsen numbers.

As the summary of this subsection, the type of solutions classified by the direction of flow ($u_r > 0$, $u_r = 0$, or $u_r < 0$) is shown on the parameter plane (Kn, $|V_{\theta 1}|/(2RT_1)^{1/2}$) in Fig. 16. There exist three types of solution at Kn = 0_+ when $|V_{\theta 1}|/(2RT_1)^{1/2} \geq \sqrt{5/2}\,[(p_{s2}/p_{s1})^{2/5} - 1]^{1/2}\,[1 - (L_1/L_2)^2]^{-1/2} = 0.5022$. Two solutions are obtained in some range of small Knudsen numbers. For the larger Knudsen numbers, there is only one solution. Bifurcation as well as reversal of a flow is seen in the second example, where the inner cylinder is rotating.

6 Concluding remarks

In the present paper, a rarefied gas between two coaxial circular cylinders made of the condensed phase of the gas was considered, where each cylinder is kept at a uniform temperature and is rotating at a constant angular velocity around its axis (cylindrical Couette flows of a rarefied gas with evaporation or condensation on the cylinders). The steady behavior of the gas was studied on the basis of kinetic theory from the continuum to the Knudsen limit. The solution showed profound variety, especially bifurcation of flow was seen even in the simple case where the state of the gas is circumferentially and axially uniform. In view of the Taylor-Couette instability of a flow, the stability of the bifurcated flows in the absence of the constraint of circumferential or axial uniformity is a problem to be studied.

Bifurcation and reversal of flow, typical features of the problem, are not special for the BKW equation. At least for the continuum limit, these are found for the standard Boltzmann equation. The fact that asymptotic analysis for small Knudsen numbers goes parallel for these equations and the physical discussion about the behavior of the gas, which is not special for the BKW model, support this.

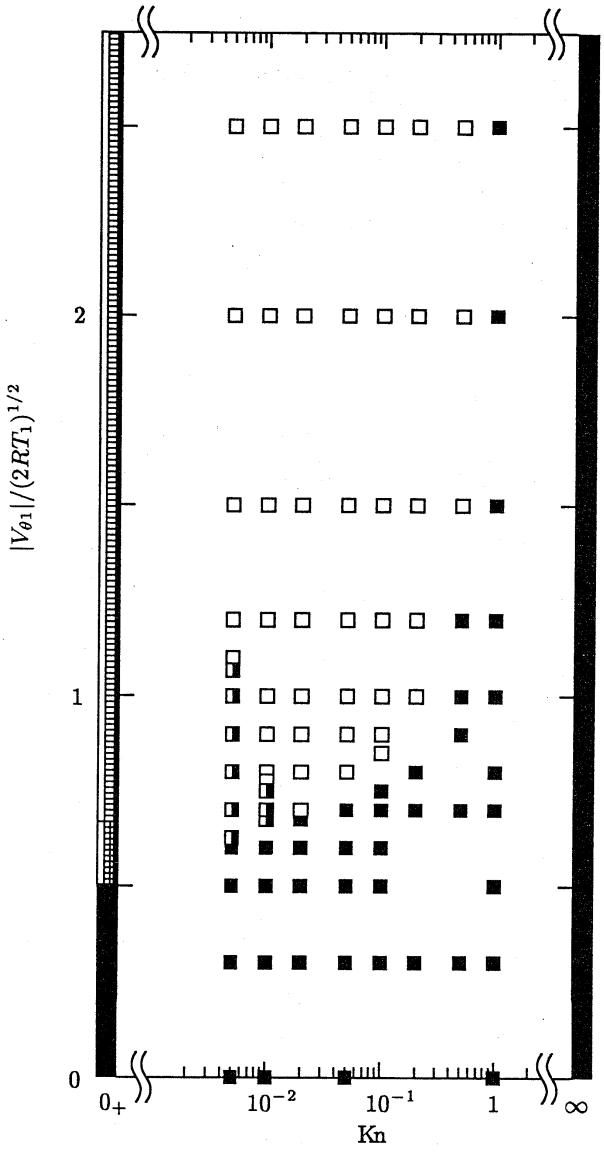

Fig. 16. The type of solution classified by the direction of flow in the plane (Kn, $V_{\theta 2}/(2RT_1)^{1/2}$) for $L_2/L_1 = 2$, $p_{s2}/p_{s1} = 1.2$, $T_2/T_1 = 1$, and $V_{\theta 2} = 0$. The symbol □ (point) and ▭ (range): a solution with $u_r > 0$; ■ (point) and ▬ (range): $u_r < 0$; ◨ : two solutions ($u_r < 0$, $u_r > 0$) exist; ▤ at Kn= 0_+: three solutions [$u_r < 0$, $u_r = 0$ ($u_r = O(\mathrm{Kn}) < 0$), $u_r > 0$] exist; ▤ at Kn= 0_+: three solutions [$u_r < 0$, $u_r = 0$ ($u_r = O(\mathrm{Kn}) > 0$), $u_r > 0$] exist.

The numerical computation was carried out on several workstations such as HP9000/C180 and VT-Alpha 533 S/N (CPU: Alpha 21164A 533MHz), and took several years of the CPU time.

References

[1] H. Bénard, "Les tourbillons cellulaires dans une nappe liquide transportant de la chaleur par convection en régime permanent," Annales Chimie Phys. **23**, 62 (1901).

[2] Lord Rayleigh, "On convective currents in a horizontal layer of fluid when the higher temperature is on the under side," Phil. Mag. **32**, 529 (1916).

[3] S. Chandrasekhar, *Hydrodynamic and Hydromagnetic Stability* (Dover, New York, 1981), Chap. II.

[4] J. S. Turner, *Buoyancy Effects in Fluids* (Cambridge Univ. Press, Cambridge, 1973).

[5] E. L. Koschmieder, *Bénard Cells and Taylor Vortices* (Cambridge Univ. Press, Cambridge, 1993), Part I.

[6] M. Nagata, "Three-dimensional finite amplitude solutions in plane Couette flow," J. Fluid Mech. **217**, 519 (1990).

[7] C. Burges and S. Zaleski, "Buoyant mixtures of cellular automaton gases," Complex Systems **1**, 31 (1987).

[8] A. Puhl, M. Malek Mansour, and M. Mareschel, "Quantitative comparison of molecular dynamics with hydrodynamics in Rayleigh-Bénard convection," Phys. Rev. A **40**, 1999 (1989).

[9] G. H. Schnerr, S. Adam, K. Lanzenberger, and R. Schulz, 'Multiphase flows: Condensation and cavitation problem," *CFD Review*, edited by M. Hafez and K. Oshima (John Wiley, Chichester, 1995), p. 614.

[10] S. Stefanov and C. Cercignani, "Monte Carlo simulation of Bénard's instability in a rarefied gas," Eur. J. Mech., B/Fluids **11**, 543 (1992).

[11] S. Stefanov and C. Cercignani, "Monte Carlo simulation of the Taylor-Couette flow of a rarefied gas," J. Fluid Mech. **256**, 199 (1993).

[12] G. A. Bird, *Molecular Gas Dynamics and the Direct Simulation of Gas Flows* (Oxford Univ. Press, 1994).

[13] Y. Sone, K. Aoki, H. Sugimoto, and H. Motohashi, "The Bénard problem of rarefied gas dynamics," in *Rarefied Gas Dynamics*, edited by J. Harvey and G. Lord (Oxford Univ. Press, Oxford, 1995), **1**, p.135.

[14] Y. Sone, K. Aoki, and H. Sugimoto, "The Bénard problem for a rarefied gas: Formation of steady flow patterns and instability of array of rolls," Phys. Fluids **10**, 3898 (1997).

[15] P. L. Bhatnagar, E. P. Gross, and M. Krook, "A model for collision processes in gases. I. Small amplitude processes in charged and neutral one-component systems," Phys. Rev. **94**, 511 (1954).

[16] P. Welander, "On the temperature jump in a rarefied gas," Ark. Fys. **7**, 507 (1954).

[17] M. N. Kogan, "On the equation of motion of a rarefied gas," Appl. Math. Mech. **22**, 597 (1954).

[18] Y. Sone and K. Aoki, *Molecular Gas Dynamics* (Asakura, Tokyo, 1994), (in Japanese).

[19] C. Cercignani, *The Boltzmann Equation and Its Applications* (Springer-Verlag, Berlin, 1988).

[20] W. B. Takkens, W. Mischke, J. Korving, and J. J. Beenakker, "A spectroscopic study of free evaporation of sodium," in *Rarefied Gas Dynamics,* edited by H. Oguchi (Univ. of Tokyo Press, Tokyo, 1984), **2**, p. 967.

[21] H. Sugimoto and Y. Sone, "Numerical analysis of steady flows of a gas evaporating from its cylindrical condensed phase on the basis of kinetic theory," Phys. Fluids A **4**, 419 (1992).

[22] Y. Sone and H. Sugimoto, "Evaporation of a rarefied gas from a cylindrical condensed phase into a vacuum," Phys. Fluids **7**, 2072 (1995).

[23] Y. Sone and S. Takata, "Discontinuity of the velocity distribution function in a rarefied gas around convex body and the S layer at the bottom of the Knudsen layer," Trans. Theory Stat. Phys. **21**, 501, (1992).

[24] K. Aoki and Y. Sone, "Gas flows around the condensed phase with strong evaporation or condensation–Fluid dynamic equation and its boundary condition in the interface and its application–," in *Advances in Kinetic Theory and Continuum Mechanics*, edited by R. Gatignol and Soubbaramayer (Springer, Berlin, 1991), p. 43.

[25] Y. Sone, S. Takata, and H. Sugimoto, "The behavior of a gas in the continuum limit in the light of kinetic theory: The case of cylindrical Couette flows with evaporation and condensation," Phys. Fluids **8**, 3403 (1996); Erratum: Phys. Fluids **10**, 1239 (1998).

[26] Y. Sone and H. Sugimoto, "Strong evaporation from a plane condensed phase," in *Adiabatic Waves in Liquid-Vapor Systems*, edited by G. E. A. Meier and P. A. Thompson (Springer, Berlin, 1990), p. 293.

[27] K. Aoki, K. Nishino, Y. Sone, and H. Sugimoto, "Numerical analysis of steady flows of a gas condensing on or evaporating from its plane condensed phase on the basis of kinetic theory: Effect of gas motion along the condensed phase," Phys. Fluids A **3**, p. 2260, (1991).

[28] H. Grad, "Singular and nonuniform limits of solutions of the Boltzmann equation," in *Transport Theory*, edited by B. Belleman, G. Birkhoff, and I. Abu-Shumays (American Mathematical Society, Providence, RI, 1969), p. 269.

[29] G. I. Taylor, "Strömung um einen Körper in einer kompression Flüssigkeit," ZAMM **10**, 334 (1930).

[30] H. Bateman, "Irrotational motion of a compressible inviscid fluid," Proc. Nat. Acad. Sci. **16**, 816 (1930).

[31] Y. Sone, "Continuum gas dynamics in the light of kinetic theory and new features of rarefied gas flows," in *Rarefied Gas Dynamics*, edited by Cheng Shen (Beijing University Press, Beijing, 1997), p. 3.

[32] Y. Sone, K. Aoki, S. Takata, H. Sugimoto, and A. V. Bobylev, "Inappropriateness of the heat-conduction equation for description of a temperature field of a stationary gas in the continuum limit: Examination by asymptotic analysis and numerical computation of the Boltzmann equation," Phys. Fluids **8**, 628 (1996).

[33] T. Ohwada, Y. Sone, and K. Aoki, "Numerical analysis of the Poiseuille and thermal transpiration flows between two parallel plates on the basis of the Boltzmann equation for hard-sphere molecules," Phys. Fluids A **1**, 2042 (1989); Erratum: Phys. Fluids A **2**, 639 (1990).